PHYSICAL REVIEW B **110**, 075150 (2024)

Influence of dark excitons on the electroabsorption spectrum of polyacetylene

Jaspal Singh Bola,[1,*] Ryan M. Stolley,[2,*] Prashanna Poudel,[1] Joel S. Miller,[2]
Christoph Boheme,[1] and Z. Valy Vardeny[1,†]
[1]*Department of Physics & Astronomy, University of Utah, Salt Lake City, Utah 84112, USA*
[2]*Department of Chemistry, University of Utah, Salt Lake City, Utah 84112, USA*

(Received 5 April 2024; revised 15 June 2024; accepted 16 July 2024; published 27 August 2024)

This study revisits the electroabsorption (EA) spectrum of polyacetylene, $(CH)_x$ thin films, for both the *cis*- and *trans*-isomers, as functions of the electric field strength, isomerization degree, and light polarization states. The EA spectrum of *cis*-$(CH)_x$ reveals an oscillatory feature that follows the Stark shift-related first derivative of the material's absorption spectrum that contains υ(0-1) and υ(0-2) sidebands of the excited C=C stretching vibration that agrees well with the Raman scattering (RS) spectrum. In contrast, the EA spectrum of *trans*-$(CH)_x$ does not match the first derivative of the material's absorption spectrum, and the phonon sideband frequency does not agree with the RS spectrum. In addition, the EA spectrum of *trans*-$(CH)_x$ reveals a band below the first allowed $1B_u$ exciton. We interpret this feature as due to the electric field activated even-parity dark (forbidden) exciton, namely mA_g ($m > 2$), showing that the "nonluminescent" *trans*-$(CH)_x$ is due to the reverse order of the excited states, where a series of dark mA_g excitons lies below the allowed $1B_u$ exciton. This agrees with the unusual phonon sideband in *trans*-$(CH)_x$ absorption, since the excited state attenuation caused by the fast internal conversion from $1B_u$ to mA_g influences the apparent frequency that determines the phonon sideband. Consequently, from the EA and RS spectra we estimate the $1B_u$ lifetime in *trans*-$(CH)_x$ to be $\sim$30 fs. Moreover, the integrated EA spectrum of *trans*-$(CH)_x$ shows a traditional Huang-Rhys type series with a relaxation parameter, $S \sim 0.5$. This indicates that the EA spectrum of the *trans* isomer is also determined by a Stark shift related to the first derivative of the absorption spectrum, but preferentially for the longest chains in the film's chain lengths distribution. This is due to the N^3 response of the nonlinear susceptibility, $\chi^{(3)}$ ($\sim$EA), dependence on the chain length having N monomers.

DOI: 10.1103/PhysRevB.110.075150

I. INTRODUCTION

Polyacetylene, $(CH)_x$, is composed of chains of carbon atoms having alternating single and double bonds that are bonded to hydrogen [see Fig. 1(a)] [1]. The double bonds exist in either *cis* or *trans* arrangements. By varying the reaction temperature, it is feasible to preferentially synthesize each isomer, namely, *cis*-polyacetylene [*cis*-$(CH)_x$] or *trans*-polyacetylene [*trans*-$(CH)_x$] [2–4]. At different synthesis temperatures, both isomers can exist simultaneously, and *cis*-$(CH)_x$ can be transformed into the more stable *trans* configuration through a heat treatment. The $(CH)_x$ chains can be as long as $\sim$100 carbon atoms, but there is a distribution of chain lengths with various monomeric units N. When synthesized, the $(CH)_x$ chains form "bundles" in the form of fibrils, which can be as long as tens of microns [see Fig. 1(b)] [4].

The *trans*-$(CH)_x$ is structurally the simplest π-conjugated polymer (PCP), with two degenerate ground states, or "A" and "B" phases, depending on the "order direction" of the single and double bonds in the chain [see Fig. 1(a)]. The misfit between the A and B phases within a chain forms a domain wall and a nonlinear shape-preserving excitation that is described by the Su, Schrieffer, and Heeger (SSH) model as a mobile soliton [5,6], which may be neutral, S^0, or charged, $S^{\pm}$. Importantly, a neutral soliton has a single electron, and, hence, a spin $s = 1/2$, whereas positively and negatively charged solitons have zero (S^+) and two electrons (S^-), respectively, which both are spinless [6–8]. This leads to the so-called excitation having "reverse spin-charge relationship," in which the charged species is spinless, whereas the spin ($s = 1/2$) carrying species is charge neutral. In particular, this model [5], which includes electron-phonon interactions, but neglects electron-electron interactions, predicts that upon a photon absorption, the photoexcited electron and hole pair is unstable, thereby relaxing within 100 fs to a charge soliton-antisoliton (S^+S^-) pair with a state in the middle of the optical gap. Within this model the nonluminescent nature of *trans*-$(CH)_x$ was taken as evidence that this process indeed dominates the photophysics of the *trans*-$(CH)_x$ isomer [9]. Little attention, however, has been devoted to the *cis*-$(CH)_x$ isomer since it has a nondegenerate structure and shows photoluminescence [9], albeit weak compared to other PCPs [10].

Over the years, the SSH model has attracted substantial attention, where both experimentalists and theoreticians have tried to prove or disprove the photogenerated S^+S^- prediction [6,11–14]. With time, however, other PCPs have been synthesized in which the photophysics is dominated by singlet and triplet excitons [11]. In a typical PCP, such as polyfluorene,

---

[*] These authors contributed equally to this work.
[†] Contact author: val@physics.utah.edu

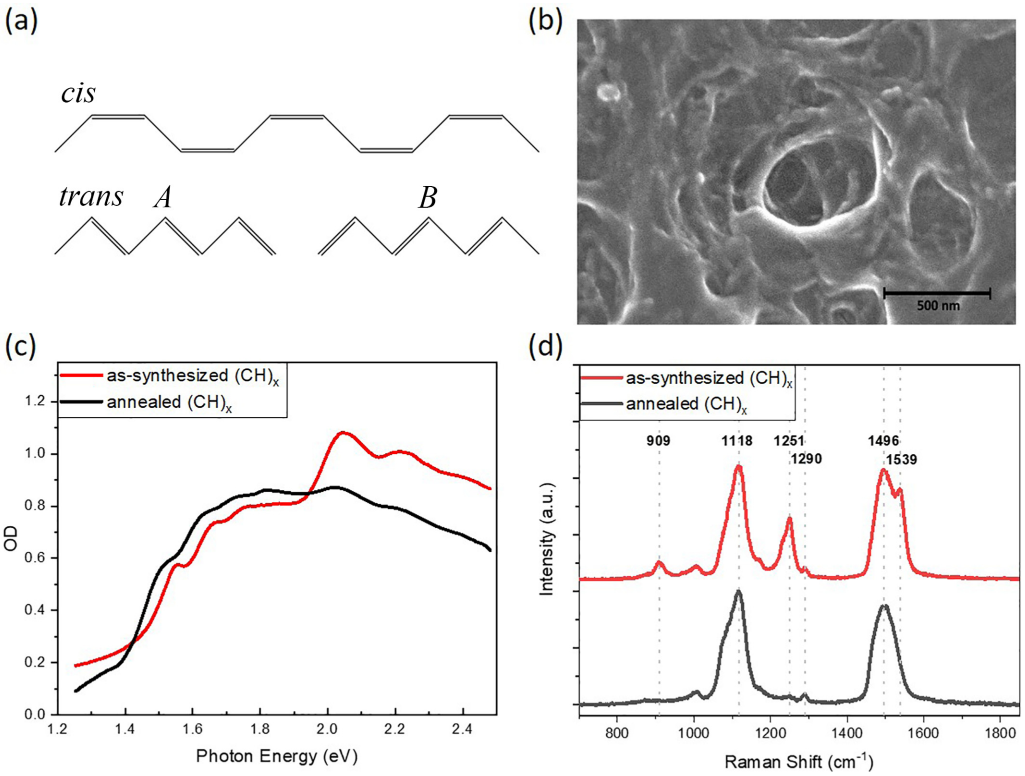

FIG. 1. (a) The *cis*- and *trans*-$(CH)_x$ structures and the two phases of the *trans*-$(CH)_x$ isomer are denoted. (b) SEM image of the fibrils in a $(CH)_x$ thin film. (c) The absorption spectrum of a $(CH)_x$ film before (red line) and after annealing (black line), plotted as optical density (OD). (d) Resonant Raman spectra of a $(CH)_x$ film before (red) and after annealing (black). A few Raman active vibrations are assigned.

polythiophene, and poly(*p*-phenylene-vinylene) derivatives, the lowest singlet exciton binding energy, namely, the $1B_u$ state, is of the order of 0.5 eV [15]. The exciton being the primary photoexcitation species in these polymers indicates that the SSH model is not suitable to describe the photophysics of most PCPs. Even for *trans*-$(CH)_x$, during the last three decades, the study of photoexcitations has revealed several unexpected phenomena, including photogeneration of a neutral excitation, which were not predicted by the SSH model [12,13]. This indicates that the nature of the primary photoexcitations in *trans*-$(CH)_x$ may be very different from the S^+S^- pair predicted by the SSH model. It is therefore expected that the electronic energy levels of *trans*-$(CH)_x$ would be also very different than that predicted by the SSH model.

An effective method to investigate the electronic energy levels in PCPs has been electroabsorption (EA) spectroscopy [16–20]. Using this technique, it is expected that the allowed excitons in PCPs, namely the B_u odd parity excitons, undergo a Stark shift which results in EA spectral features that resemble the first-derivative of the absorption spectrum [21,22]. Also, the forbidden (or dark) excitons with the A_g even parity would become partially allowed due to the symmetry breaking imposed by the external electric field [22]. EA spectroscopy is a very useful method to study whether the $1B_u$ exciton is indeed the lowest exciton in a specific PCP [23], or alternatively there is an A_g state (mA_g, where $m > 1$ is an integer) below it. Kasha's rule states that photoluminescence (PL) at steady state is mainly due to the lowest energy excited state of the material. Accordingly, if the $1B_u$ is indeed the lowest exciton, then the PCP is luminescent; however, if $E(1B_u) > E(2A_g)$, then the specific PCP is nonluminescent. Since *trans*-$(CH)_x$ is nonluminescent, whereas *cis*-$(CH)_x$ is luminescent, it is important to revisit EA spectroscopy of $(CH)_x$ [20,24,25], in order to corroborate that this material can be described by the same theoretical framework as many other PCPs, without invoking an ultrafast generation of S^+S^- excitation to explain the apparent lack of PL in this polymer. This is particularly important as, upon deposition of a $(CH)_x$ film, the materials contains both *trans* and *cis* isomers, which are nonluminescent and luminescent, respectively.

In the study presented here, we report the synthesis and investigation of $(CH)_x$ films using optical absorption, EA and Raman scattering (RS) spectroscopies, at different stages of the $(CH)_x$ isomerization, with the goal to scrutinize the EA spectra of the luminescent *cis*-$(CH)_x$ and nonluminescent *trans*-$(CH)_x$ for the first derivative of the material's absorption spectrum.

II. EXPERIMENTAL PROCEDURES

The procedure employed for synthesizing the polyacetylene $(CH)_x$ thin films in this study was a modified version of the method reported by Shirakawa and co-workers in 1999 [26], as detailed in the Supplemental Material (SM) [27]. The synthesis of the polymerization catalyst was prepared using a freshly prepared catalyst solution (0.003 M) synthesized by the addition of tetra-*n*-butoxytitanium(IV) (Thermo-Fisher), $Ti(OBu)_4$ (251 μL, 0.74 mmol, 1 equiv), to a 1-M solution of triethylaluminium, $AlEt_3$ (Sigma Aldrich) in hexanes (2.95 mL, 2.95 mmol, 4.0 equiv) under Schlenk conditions. The resulting solution was heated to 150 °C for 1 h, then allowed to cool to room temperature affording a 0.1-M solution. The catalyst solution was then dissolved in dry, degassed toluene (Thermo-Fisher) to the appropriate polymerization concentration. The polymerization process utilized high purity acetylene gas (Airgas, 99.6%) dissolved in acetone that was further purified by washing through subsequent stages of saturated sodium bisulfite, concentrated sulfuric acid, and passage through packed columns of activated alumina and Drierite®. Thin films of $(CH)_x$ having various thicknesses were deposited on different substrates such as quartz, sapphire, and KBr within a controlled nitrogen and/or acetylene environment. Each substrate was dried in an oven prior to deposition and placed in a pre-dried Schlenk flask equipped with a rubber septum and attached to an appropriately outfitted manifold. Under a nitrogen atmosphere, the catalyst solution was deposited onto the substrate and the atmosphere exchanged for acetylene. Upon exchanging the atmosphere, an immediate formation of the purple polymerization product was apparent. Upon deposition of the desired thickness, the atmosphere was evacuated and the substrate was dried under vacuum. The films were then washed under nitrogen with toluene (3 × 1–2 mL) and dried thoroughly under vacuum. The film thicknesses were then determined by using the well-known optical density strength [28], which turned out to be in a range ~100 nm to 1 μm. Isomerization from the as-synthesized film by converting the *cis*-$(CH)_x$ chains in the films into *trans*-$(CH)_x$ chains was done by heating the film while being sealed in a nitrogen environment at a temperature of 150 °C, and various durations (~tens of min), depending on the desired *cis*-$(CH)_x$/*trans*-$(CH)_x$ ratio.

The optical absorption spectra for the deposited thin films were measured using an in-house setup containing a 1/4 met. monochromator with a tungsten lamp that serves as the incident light source directed onto the sample. The thin $(CH)_x$ film was placed in a cryostat capable of maintaining temperatures between 10 and 300 K. The transmitted light intensity was measured using a silicon detector. The Raman scattering spectra were obtained in reflection mode using a 488-nm laser at low intensity at room temperature, using a 1/4 met. monochromator with spectra measured from 400 to 1900 cm^{-1} with a resolution of 2 cm^{-1}.

The EA measurements were conducted on various thin $(CH)_x$ films having different *cis*-$(CH)_x$/*trans*-$(CH)_x$ ratios, deposited on sapphire substrates with patterned metallic, interdigited electrodes, consisting of several hundred, 10-micrometer-wide gold strips [19]. The EA measurement setup is shown in SM Fig. S1 [27]. The devices were placed in a cryostat for low temperature measurements. By applying a potential V to the electrodes, in-plane electric field on the order of $F \approx 10^5$ V/cm was generated. Typically, a voltage $V = 300$ V was applied at a modulation frequency $f = 1$ kHz. To probe the EA spectrum, we used an incandescent light source from a tungsten lamp, which was dispersed through a 1/4 met. monochromator, focused on the sample, and detected by a silicon photodiode. For the EA experiments, we measured the changes ΔT in the transmission spectrum T using a lock-in amplifier, set to twice the frequency ($2f$) of the applied modulation frequency, and verified that no EA signal was observed at f or $3f$ [see SM Fig. S2(a)]. The spectra of ΔT and T were measured separately, using the same setup, and the EA spectrum was subsequently obtained from the spectral ratio $\Delta T/T$.

III. RESULTS AND DISCUSSION

The optical absorption spectra of both an "as-synthesized" $(CH)_x$ film and another film that underwent annealing at 150 °C for 30 min, where the *cis*- to *trans*-$(CH)_x$ isomerization occurs, are shown in Fig. 1(c). The absorption spectrum of the as-synthesized film shows two superimposed bands having onset at 1.4 and 2.0 eV, respectively. Upon isomerization from *cis* to *trans*, the higher energy band weakens, and thus it is identified as the absorption band of *cis*-$(CH)_x$ with an optical gap of ~2 eV. This is in agreement with the PL spectrum of *cis*-$(CH)_x$ that was measured to peak at 1.97 eV [28]. Consequently, the low energy absorption band is due to the *trans*-$(CH)_x$ isomer in the film with an optical gap at ~1.4 eV depending on the *trans/cis* ratio that is consistent with an extremely weak polarized PL band at 1.41 eV having a phonon sideband at 1.37 eV [14]. Note that each absorption band also contains several superimposed weaker features. These are phonon sidebands of the lowest lying allowed exciton in these two isomers, which become more visible in the EA spectra (see below). The broad absorption band of the *trans* isomer indicates that the *trans* chains in the film have a broad distribution of chain lengths. This reflects that the energy, $E(N)$, of lowest allowed $1B_u$ exciton of the *trans* chains (i.e., polyenes) that depends on the chain length N as $E(N) = E_{\min} + a/N$ where a is a constant and $E_{\min}$ is the exciton energy of the longest chain length [29,30]. This broadens the phonon sidebands, as noted in the absorption spectra. Another contribution to the broad absorption band related to *trans*-$(CH)_x$ isomer may be attributed to scattering from the $(CH)_x$ fibrils [24] [Fig. 1(b)].

The resonant Raman scattering (RRS) of the as-synthesized film and the "annealed" $(CH)_x$ film are shown in Fig. 1(d). The RRS spectrum of as-synthesized film contains three resonantly enhanced Raman bands at 909, 1251, and 1539 cm^{-1}, which diminish upon isomerization. We assign this trio of Raman bands to the C-C stretching, C-C bending, and C=C stretching modes, respectively, of *cis*-$(CH)_x$, in agreement with the literature [31]. The other three bands in the RRS spectrum of the as-synthesized film are observed at 1118, 1290, and 1496 cm^{-1} and do not disappear upon isomerization; thus, they are also assigned to the C-C stretching, C-C bending, and C=C stretching vibrations, respectively, of the *trans*-$(CH)_x$ chains, as assigned in the literature [32]. Interestingly, the phonon sidebands in the *cis*-$(CH)_x$ absorption spectrum are dominated by the excited state C=C stretching vibration at ~1540 cm^{-1}. In contrast, the *trans*-$(CH)_x$ phonon sidebands do not fit any of the resonantly enhanced vibrations of the *trans*-$(CH)_x$ isomer as measured by the RS spectrum [Fig. 1(d) and [32]].

The 80-K EA spectra for the as-synthesized and annealed $(CH)_x$ films are compared with their respective absorption spectra in Figs. 2(a) and 2(b), respectively. We note that the EA spectra are free from the assumed background absorption due to light scattering that may be included in the

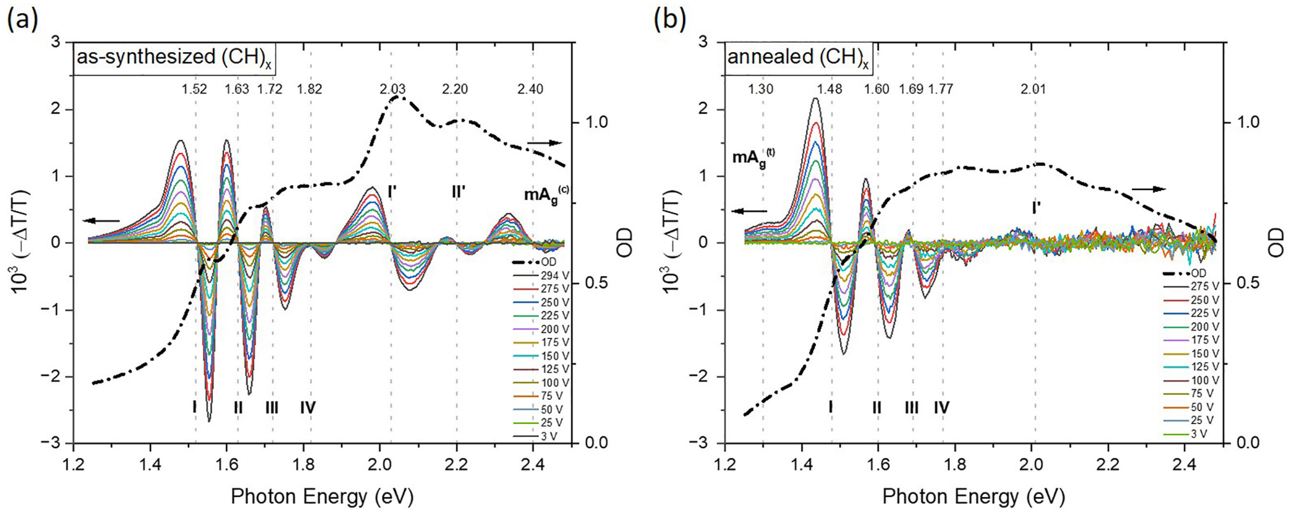

FIG. 2. The electroabsorption (EA) spectra for various applied voltages compared with the absorption spectra (OD) (•-•) for as synthesized (a) and annealed (b) $(CH)_x$ thin film. The zero-crossing photon energies, I–IV, and the $mA_g^{(t)}$ band are assigned for the *trans*-$(CH)_x$ isomer; and I′, II′, and $mA_g^{(c)}$ are assigned for the *cis*-$(CH)_x$ isomer.

obtained "absorption" spectrum [24] [see Fig. 1(c)]. In the as-synthesized film, we observe an oscillatory feature above 1.9 eV that diminishes upon annealing. This supports the assignment that these oscillatory bands with "zero crossing" at 2.03, 2.20, and 2.40 eV, respectively (labeled I′, II′, and $mA_g^{(c)}$ [22] respectively), correspond to the *cis*-$(CH)_x$ isomer. As for the oscillation with zero crossing at 1.52, 1.63, 1.72, and 1.82 eV, respectively (labeled I, II, III, and IV, respectively), in the as-synthesized film, we note that similar features, albeit redshifted, are also seen in the annealed film with zero crossing at 1.48, 1.60, 1.69, and 1.77 eV, respectively; we thus assign these oscillatory features as due to the *trans*-$(CH)_x$ isomer in the film.

The EA spectrum of the annealed film also contains a band below the first oscillation feature that appears to be a single peak at 1.32 eV. This band does not have any contribution in the absorption spectrum of the film. It has been well studied that the $2A_g$ state has very little contribution in nonlinear optical spectra, including in the EA spectrum [33–35] and therefore we assign it to an even parity dark (forbidden) exciton, mA_g ($m > 2$) that is activated by the electric field, which in fact breaks the inversion symmetry in the film [22]. This A_g state is close, but still below the absorption edge; as such, it serves as an "energy sink" for the photogenerated $1B_u$ exciton in the *trans*-$(CH)_x$ chains according to Kasha's thermalization rule. This may explain the extremely weak PL emission spectrum of the *trans*-$(CH)_x$ isomer [14], and serves as a straightforward explanation of the nonluminescent nature of this isomer without invoking photogenerated charged soliton pairs using the SSH model [9].

Since the EA spectrum accentuates the oscillatory feature related to the phonon sidebands arising from the vibronic coupling with an excited state vibration, it is easy to see that the energy period, ΔE in the *cis*-$(CH)_x$ part of the spectrum, is $\sim 185 \pm 15$ meV ($\sim 1480 \pm 120\,\mathrm{cm}^{-1}$), which is in fair agreement with the C=C stretching mode frequency (1539 cm^{-1}) of this isomer obtained from the RRS spectrum [Fig. 1(d)]. In contrast, ΔE in the *trans*-$(CH)_x$ part of the EA spectrum is 95 ± 15 meV ($\sim 760 \pm 120\,\mathrm{cm}^{-1}$) which does not correspond to any of the Raman modes revealed in the RRS spectrum [see Fig. 1(d)]; in particular it is much lower than the most strongly coupled C=C stretching vibration of the *trans* isomer obtained in the RRS spectrum at 1495 cm^{-1} [Fig. 1(d)]. We believe that this discrepancy is due to the large attenuation coefficient γ in the excited state vibrational mode related to the $1B_u$ exciton in *trans*-$(CH)_x$ due to the fast decay into the mA_g exciton that lies close but below it in this isomer. In this case we may use a simplified "damped harmonic oscillator" equation [36],

$$(\nu_{ap})^2 = (\nu_0)^2 - \gamma^2, \tag{1}$$

where $\nu_{ap}(=760\,\mathrm{cm}^{-1})$ is the observed or "apparent" frequency and $\nu_0(=1495\,\mathrm{cm}^{-1})$ is the unperturbed frequency. Using Eq. (1) we calculate the attenuation $\gamma = 1287\,\mathrm{cm}^{-1}$ (or ~39 THz). From the relation $\gamma = \tau^{-1}$ where τ is the $1B_u$ lifetime, we estimate $\tau = 26$ fs. This short lifetime is in agreement with the $1B_u$ exciton lifetime estimated directly from the ultrafast transient photoinduced absorption measured in *trans*-$(CH)_x$ [14]. We may also apply Eq. (1) to estimate the $1B_u$ exciton lifetime in *cis*-$(CH)_x$. From the comparison between the phonon sidebands, namely, ν_{ap} (1480 cm^{-1}), and the C=C stretching vibration, $\nu_0(=1539\,\mathrm{cm}^{-1})$ measured in the RS spectra, $\gamma = 422\,\mathrm{cm}^{-1}$ that leads to $\tau = 78$ fs. This value represents the time during which the photogenerated exciton in *cis*-$(CH)_x$ chains in the film decays into the excited states manifold of the lower energy *trans*-$(CH)_x$ chains and explain the stronger PL emission of this isomer. We note that the two τ values are given in Table I. We can then calculate the *QE* of the PL from the relation $QE = \tau/(\tau + \tau_{rad})$, where τ_{rad} is the radiative lifetime which for $1B_u$ exciton is ~1 ns. Consequently from the above relation, the *QE* of the PL in both *cis*- and *trans*-$(CH)_x$ is of the order of 10^{-4}.

Figures 3(a) and 3(b) show the EA amplitude versus the applied voltage V that follows a quadratic (V^2) response,

TABLE I. The energies of the peaks in the integrated EA spectra of the as-synthesized and annealed $(CH)_x$ films. Peaks I–IV stand for the *trans*-$(CH)_x$ and peaks I′–III′ are for the *cis*-$(CH)_x$. The Huang Rhys parameter S is also given.

$EA(CH)_x$	As-synthesized peak center (eV)	Annealed peak center (eV)
Peak I	1.52	1.48
Peak II	1.63	1.60
Peak III	1.72	1.69
Peak IV	1.82	1.77
Peak I′	2.03	2.01
Peak II′	2.20	2.18
Peak III′	2.40	2.41
S parameter-*trans*	0.49	0.54
S parameter-*cis*	0.22	0.66

which is the leading EA term when the material has inversion symmetry, such as the $(CH)_x$ chains. Figure 3(c) compares the EA spectrum to that of the absorption derivative spectrum. The EA spectrum of *cis*-$(CH)_x$ follows the Stark shift-related first derivative of the absorption spectrum that contains $v(0\text{-}0)$, $v(0\text{-}1)$, and $v(0\text{-}2)$ phonon sidebands. We note that the absorption derivative spectrum contains a contribution from the scattered light that does not show in the EA spectrum, so the broad EA spectrum cannot be compared to the absorption derivative spectrum within the spectral range of this spectral feature [19,37].

Figure 3(d) shows the light polarization dependence of the EA spectrum. Horizontal polarized light is oriented along the direction x of the applied electric field in the EA measurement. The EA magnitude in the x direction is twice larger than that in the y direction. This is the consequence of the EA being a nonlinear optical process. In fact, the EA is related to the imaginary part of the third order susceptibility tensor, $\mathrm{Im}\chi^{(3)}(0, 0, \omega, -\omega)$. Since $\chi^{(3)}$ is a third order tensor, it contains four indexes, namely, χ_{ijkl}. Consequently, the obtained light polarization dependence indicates that $\chi_{\mathrm{xxyy}} = \frac{1}{2}\chi_{\mathrm{xxxx}}$, which is the case when the $(CH)_x$ fibrils are randomly oriented in the plane of the polyacetylene film [20].

To better understand the EA spectrum in $(CH)_x$, we need to identify its origin. Since the EA spectra should show a Stark

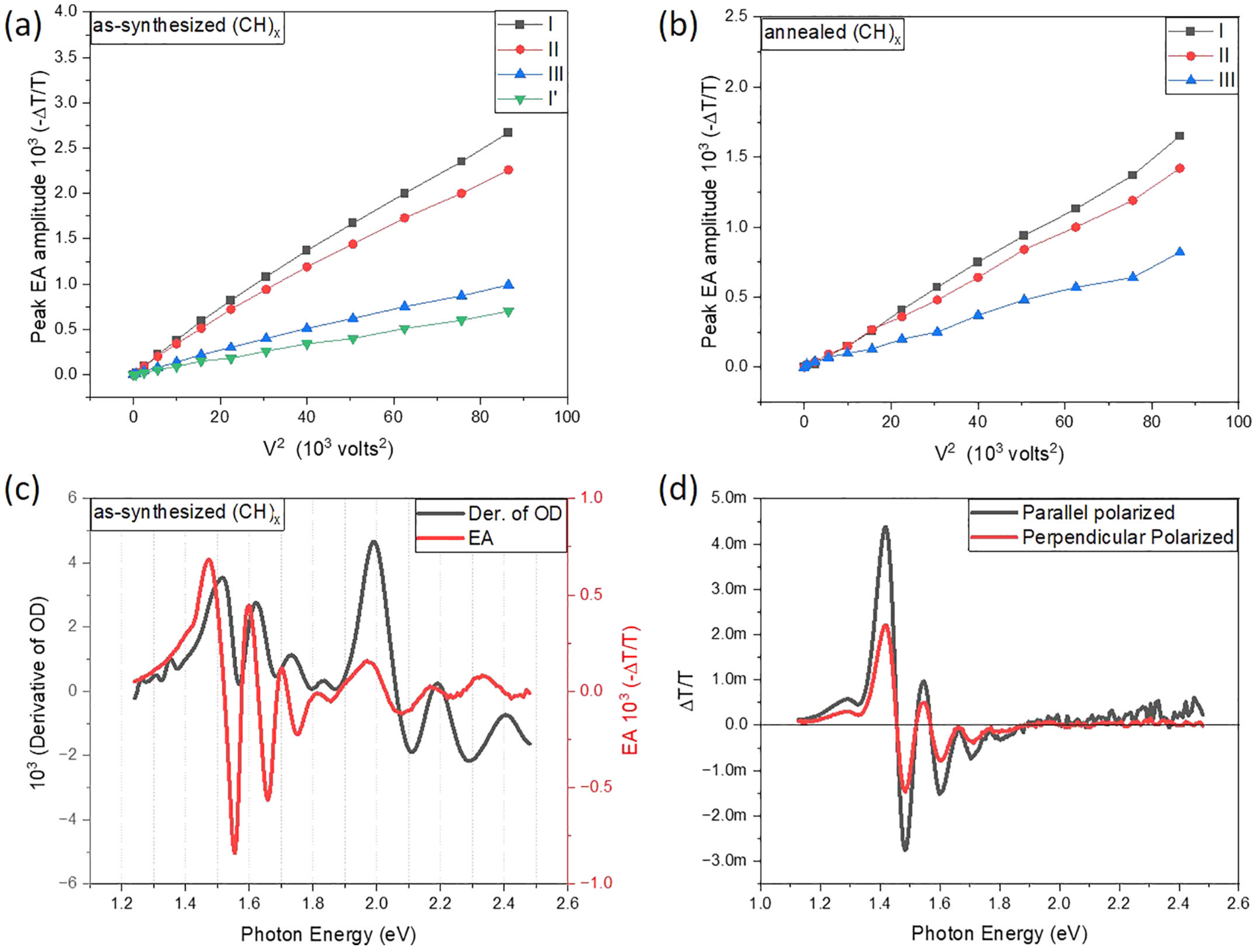

FIG. 3. The EA strengths vs V^2 for the as-synthesized (a) and annealed (b) $(CH)_x$ films at several photon energies that correspond to peaks in the EA spectra as denoted in Fig. 2(a). (c) Comparison between the EA spectrum and the derivative (Der) of the absorption spectrum for the as-synthesized $(CH)_x$ film. (d) The EA spectra of a $(CH)_x$ film measured at two different light polarization, namely, parallel (black) and perpendicular (red) to the applied electric field.

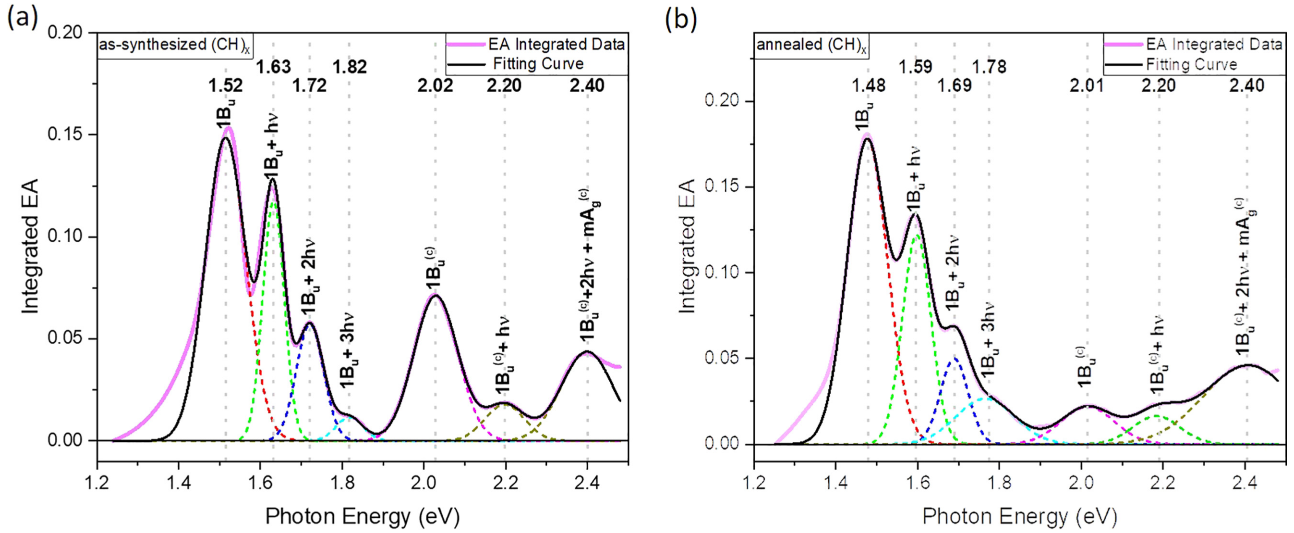

FIG. 4. The integrated EA spectra of (a) the as-synthesized and (b) the annealed $(CH)_x$ film. Various bands and phonon replica are assigned (see Table I). The broken lines through the data are a fit using the Huang-Rhys model [Eq. (2)].

shift, a useful way to get the spectrum of the EA source is to integrate the EA spectra for the two isomers. The integrated spectra are shown for the as-synthesized and annealed films in Figs. 4(a) and 4(b), respectively, and the resulting peaks are summarized in Table I. The EA and integrated spectra for different annealing times are shown in SM Figs. S3 and S4, respectively, showing that the integrated EA spectrum of the *cis*-$(CH)_x$ resembles its absorption spectrum, except for the band at 2.4 eV, where it is stronger than what would be anticipated for a simple phonon υ(0-2) sideband. We thus identify this band in the EA spectrum as due to a superposition of the second phonon sideband of the $1B_u$ exciton at 2.02 eV and an even parity state (namely, mA_g) that is activated by the applied electric field. We note that the energy difference between the $1B_u$ and mA_g exciton in *cis*-$(CH)_x$ (~0.4 eV) is similar to many other luminescent PCPs [37,38]. We therefore conclude that *cis*-$(CH)_x$ falls in the class of nondegenerate luminescent PCPs.

In contrast, the integrated EA spectrum of the *trans*-$(CH)_x$ isomer in the film [Fig. 4(b)] is much narrower than the respective absorption spectrum [see Fig. 1(c)]. It shows a $1B_u$ band followed by three phonon sidebands. We note that the $1B_u$ energy redshifts from 1.52 to 1.48 eV upon annealing. This indicates that the *trans*-$(CH)_x$ chains become longer upon isomerization [1,36,39]. We can fit the integrated EA spectra of the *trans* and *cis* isomers using the Huang Rhys model:

$$\alpha(\omega) \sim \left[e^{-S} \sum_{p=0}^{\infty} \frac{S^p}{p!} \frac{1}{\left(E_{1B_u} + ph\nu - h\omega\right)} \right], \tag{2}$$

where S is the Huang Rhys (HR) parameter that determines the relative strength of the successive phonon sidebands and $h\nu$ is the apparent vibration energy. As seen in Table I, S for the *trans*-$(CH)_x$ isomer is ~0.5 that is much larger than S for the *cis* isomer. The relaxation energy E_r of the $1B_u$ exciton is determined by the S parameter via $E_r = Sh\nu_0$, where ν_0 is the vibration frequency of the most coupled phonon, namely, the C=C stretching mode. Taking the C=C stretching mode energy of 190 meV (1532 cm^{-1}), we get $E_r = 93\,\text{meV}$ ($750\,\text{cm}^{-1}$). From the EA at room temperature we determined that the $1B_u$ exciton is at $E(1B_u) = 1.53\,\text{eV}$ ($12340\,\text{cm}^{-1}$). Hence, the photoluminescence band calculated from $E(1B_u) - E_r = 1.44\,\text{eV}$ ($11615\,\text{cm}^{-1}$), which matches the PL band measured at room temperature in *trans*-$(CH)_x$ by Sheng *et al.* [14].

The reason that the integrated EA spectrum of *trans*-$(CH)_x$ is much narrower than the absorption spectrum is the chain length dependence of the nonlinear susceptibility in PCPs, namely, $\chi^{(3)} \sim N^3$, where N is the number of C-H units in the polymer chain [19,22]. Therefore, the EA accentuates the longest chains in the film as is evident from the integrated EA spectrum. This solves the puzzle of the EA spectrum in *trans*-$(CH)_x$ that has remained in the field for about three dozen years [20,24,25]. There is no need to relate the EA spectrum to the second derivative of the absorption spectrum as done in a previous study [20]. Hence, the shorter chains in the chain length distribution do not contribute equally to the EA spectrum. This explanation may be also true for the EA spectra of the entire class of the PCPs.

IV. CONCLUSIONS

We presented the EA spectra of *cis*- and *trans*-$(CH)_x$ in films of different *cis*-/*trans*-$(CH)_x$ ratios, light polarization, and electric field dependence. The EA spectrum of the *cis* isomer can be described by a Stark-shift related first derivative of its absorption spectrum. In contrast to the conclusions of previous works, the EA spectrum of the *trans* isomer can also be described as a first derivative of the absorption spectrum, but of the longest chains in the film. In addition, the EA spectrum of *trans*-$(CH)_x$ reveals a dark mA_g ($m > 2$) state that lies below the allowed $1B_u$ exciton. From the comparison of the phonon sidebands revealed in the EA spectrum and the RRS spectrum that are dominated by the C=C stretching vibration, we estimate the internal conversion time of $1B_\mathrm{u} \rightarrow mA_\mathrm{g}$ to be of the order of 30 fs. This explains the nonluminescent character of *trans*-$(\mathrm{CH})_\mathrm{x}$ without the need to involve ultrafast charge solitons photogeneration.

ACKNOWLEDGMENTS

This work was supported by NSF Grant No. DMR-2206653. We also acknowledge the Dixon Laser Institute of the University of Utah's Department of Physics & Astronomy for instrumentation support.

---

[1] J. C. W. Chien, *Polyacetylene: Chemistry, Physics, and Material Science* (Academic, Orlando, FL, 1984).

[2] A. M. Saxman, R. Liepins, and M. Aldissi, Polyacetylene: Its synthesis, doping and structure, Prog. Polym. Sci. **11**, 57 (1985).

[3] W. J. Feast, J. Tsibouklis, K. L. Pouwer, L. Groenendaal, and E. W. Meijer, Synthesis, processing and material properties of conjugated polymers, Polymer **37**, 5017 (1996).

[4] D. J. Berets and D. S. Smith, Electrical properties of linear polyacetylene, Trans. Faraday Soc. **64**, 823 (1968).

[5] W. P. Su, J. R. Schrieffer, and A. J. Heeger, Solitons in polyacetylene, Phys. Rev. Lett. **42**, 1698 (1979).

[6] A. J. Heeger, S. Kivelson, J. R. Schrieffer, and W.-P. Su, Solitons in conducting polymers, Rev. Mod. Phys. **60**, 781 (1988).

[7] Z. Vardeny and J. Tauc, Method for direct determination of the effective correlation energy of defects in semiconductors: Optical modulation spectroscopy of dangling bonds, Phys. Rev. Lett. **54**, 1844 (1985).

[8] Z. Vardeny and J. Tauc, Vardeny and tauc response, Phys. Rev. Lett. **56**, 1510 (1986).

[9] W. P. Su and J. R. Schrieffer, Soliton dynamics in polyacetylene, Proc. Natl. Acad. Sci. USA **77**, 5626 (1980).

[10] Z. H. Kafafi, *Organic Photovoltaics XVII* (SPIE - International Society for Optics and Photonics, San Diego, 2016).

[11] S. Mazumdar and M. Chandross, Theory of excitons and biexcitons in pi-conjugated polymers, in *Primary Photoexcitations in Conjugated Polymers: Molecular Exciton Versus Semiconductor Band Model*, edited by N. S. Sariciftci (World Scientific, Hackensack, NJ, 1997).

[12] X. Wei, B. C. Hess, Z. V. Vardeny, and F. Wudl, Studies of photoexcited states in polyacetylene and poly(paraphenylenevinylene) by absorption detected magnetic resonance: The case of neutral photoexcitations, Phys. Rev. Lett. **68**, 666 (1992).

[13] M. L. Tiago, M. Rohlfing, and S. G. Louie, Bound excitons and optical properties of bulk trans-polyacetylene, Phys. Rev. B **70**, 193204 (2004).

[14] C. X. Sheng, K. H. Kim, M. Tong, C. Yang, H. Kang, Y. W. Park, and Z. V. Vardeny, Ultrafast transient spectroscopy of trans-polyacetylene in the midinfrared spectral range, Phys. Rev. Lett. **124**, 017401 (2020).

[15] H. Zhao, S. Mazumdar, C.-X. Sheng, M. Tong, and Z. V. Vardeny, Photophysics of excitons in quasi-one-dimensional organic semiconductors: Single-walled carbon nanotubes and π-conjugated polymers, Phys. Rev. B **73**, 075403 (2006).

[16] L. Sebastian and G. Weiser, Electric field modulated spectra of polydiacetylene single crystal (PTS), Chem. Phys. Lett. **64**, 396 (1979).

[17] L. Sebastian and G. Weiser, Electroreflectance studies on the excitons in PTS and DCHD single crystals, Chem. Phys. **62**, 447 (1981).

[18] L. Sebastian and G. Weiser, One-dimensional wide energy bands in a polydiacetylene revealed by electroreflectance, Phys. Rev. Lett. **46**, 1156 (1981).

[19] M. Liess, S. Jeglinski, Z. V. Vardeny, M. Ozaki, K. Yoshino, Y. Ding, and T. Barton, Electroabsorption spectroscopy of luminescent and nonluminescent π-conjugated polymers, Phys. Rev. B **56**, 15712 (1997).

[20] S. D. Phillips, R. Worland, G. Yu, T. Hagler, R. Freedman, Y. Cao, V. Yoon, J. Chiang, W. C. Walker, and A. J. Heeger, Electroabsorption of polyacetylene, Phys. Rev. B **40**, 9751 (1989).

[21] M. Cardona, *Solid State Physics Supplement 11: Modulation Spectroscopy* (Academic, New York, 1969).

[22] D. Guo, S. Mazumdar, S. N. Dixit, F. Kajzar, F. Jarka, Y. Kawabe, and N. Peyghambarian, Role of the conduction band in electroabsorption, two-photon absorption, and third-harmonic generation in polydiacetylenes, Phys. Rev. B **48**, 1433 (1993).

[23] A. Horvath, G. Weiser, C. Lapersonne-Meyer, M. Schott, and S. Spagnoli, Wannier excitons and Franz-Keldysh effect of polydiacetylene chains diluted in their single crystal monomer matrix, Phys. Rev. B **53**, 13507 (1996).

[24] J. Orenstein, G. L. Baker, and Z. Vardeny, Photogenerated gap states in polyacetylene, J. Phys. Colloq. **44**, C3 (1983).

[25] T. W. Hagler and A. J. Heeger, Soliton-antisoliton configurations and the linear and nonlinear optical response of degenerate-ground-state conjugated polymers, Phys. Rev. B **49**, 7313 (1994).

[26] T. S. Liang, K. Akagi, and H. Shirakawa, Synthesis of polyacetylene ultra-thin film, Synth. Met. **101**, 67 (1999).

[27] See Supplemental Material at http://link.aps.org/supplemental/10.1103/PhysRevB.110.075150 for synthesis of polyacetylene films; electroabsorption spectroscopy setup; EA and integrated EA spectra for various annealing time.

[28] L. Lauchlan, S. Etemad, T.-C. Chung, A. J. Heeger, and A. G. MacDiarmid, Photoexcitations in polyacetylene, Phys. Rev. B **24**, 3701 (1981).

[29] B. E. Kohler, The polyene $2\,^1A_g$ state in polyacetylene photoinduced absorption and thermal isomerization, J. Chem. Phys. **88**, 2788 (1988).

[30] B. E. Kohler, A simple model for linear polyene electronic structure, J. Chem. Phys. **93**, 5838 (1990).

[31] H. Kuzmany, Resonance Raman scattering from neutral and doped polyacetylene, Phys. Status Solidi B **97**, 521 (1980).

[32] E. Ehrenfreund, Z. Vardeny, O. Brafman, and B. Horovitz, Amplitude and phase modes in trans-polyacetylene: Resonant Raman scattering and induced infrared activity, Phys. Rev. B **36**, 1535 (1987).

[33] S. N. Dixit, D. Guo, and S. Mazumdar, Essential-states mechanism of optical nonlinearity in Π-conjugated polymers, Phys. Rev. B **43**, 6781 (1991).

[34] S. Mazumdar and F. Guo, Observation of three resonances in the third harmonic generation spectrum of conjugated polymers:

Evidence for the four-level essential states model, J. Chem. Phys. **100**, 1665 (1994).

[35] M. Liess, S. Jeglinski, P. A. Lane, and Z. V. Vardeny, A three essential states model for electroabsorption in non-luminescent π-conjugated polymers, Synth. Met. **84**, 891 (1997).

[36] C. C. Wu, E. Ehrenfreund, J. J. Gutierrez, J. P. Ferraris, and Z. V. Vardeny, Apparent vibrational side bands in π-conjugated systems: The case of distyrylbenzene, Phys. Rev. B **71**, 081201(R) (2005).

[37] Z. G. Soos, D. Mukhopadhyay, and M. H. Hennessy, Stark profiles of singlet excitons in conjugated polymers, Chem. Phys. **210**, 249 (1996).

[38] Z. G. Soos, D. S. Galvão, and S. Etemad, Fluorescence and excited-state structure of conjugated polymers, Adv. Mater. **6**, 280 (1994).

[39] S. Jeglinski and Z. V. Vardeny, Electroabsorption in polydiethynylsilane and soluble $trans$-(CH)$_x$, Synth. Met. **50**, 509 (1992).